Comparative Study of Homogenization Techniques for Evaluating the Bearing Capacity of Bimsoils under Shallow Foundations

Silvana Montoya Noguera, Fernando Lopez-caballero

Comparative Study of Homogenization Techniques for Evaluating the Bearing Capacity of Bimsoils under Shallow Foundations

Silvana Montoya-Noguera[a,*], Fernando Lopez-Caballero[b]

[a] *Applied Mechanics Research Group, School of Applied Sciences and Engineering, Universidad EAFIT, Medellín, Colombia*
[b] *Laboratoire de Mécanique Paris-Saclay, Université Paris-Saclay, CentraleSupélec, ENS Paris-Saclay, 91190 Gif-Sur-Yvette, France*

Abstract

Bimsoils, characterized by discrete blocks within a finer-grained matrix, pose challenges in evaluating the bearing capacity of shallow foundations due to their spatial variability. To address this, a binary random field coupled with a Finite-Element model is used to simulate the variability of bimsoils. This study focuses on investigating the effect of the blocks spatial fraction (γ), the isotropic and anisotropic spatial correlations, and the undrained shear strength (c_u) ratio between the matrix and the blocks. The results reveal that the coefficients of variation (CV) for the bearing capacity (q_u), at a given γ, reach nearly 20% due to the diverse spatial configurations. This dispersion is attributed to the development of distinct failure mechanisms. However, optimizing the local average area used to evaluate γ can help reduce these CV values. The average q_u for a given γ can be accurately determined using the Bruggeman symmetric effective medium (BEM) equation, ensuring safe design compared to traditional homogenization techniques. The BEM equation considers γ and the c_u ratio, providing an accurate estimation of bearing capacity for an equivalent homogeneous model suitable for probabilistic analyses.

Keywords: Bimsoils, Spatial variability, Binary random fields, Bearing capacity, Homogenization theories, Finite element model

1. INTRODUCTION

Bimsoils (Block-in-Matrix soils), consisting of geotechnically complex formations, present unique challenges in civil engineering due to their heterogeneous nature and spatial variability of mechanical parameters (Napoli et al., 2022). The interaction between the blocks and the matrix, along with their contrasting geotechnical parameters, necessitates the development of appropriate homogenization techniques to accurately evaluate the bearing capacity of these soils.

*Corresponding author
Email address: smontoyan@eafit.edu.co (Silvana Montoya-Noguera)

Conventional geotechnical analyses often oversimplify bimsoils by assuming homogeneity, disregarding the inherent complexities arising from the presence of discrete blocks within the matrix. Some authors have suggested using only the shear strength parameters derived from the weaker matrix when the spatial fraction of blocks is small (Medley, 2001; Medley and Sanz Rehermann, 2004). This simplified approach can lead to inaccurate predictions, excessively conservative designs and compromised safety margins. Lindquist (1994) and Sonmez et al. (2009), among others, proposed statistical relationships to adjust the values of uniaxial compressive strength, friction angle and cohesion for bimsoils by utilizing their matrix values as a function of the spatial fraction. The mechanical influence of increasing the spatial fraction primarily arises from the formation of tortuous failure surfaces that circumnavigate the blocks. The following has been studied on the effect of slope stability by Medley and Sanz Rehermann (2004) and Montoya-Araque et al. (2020), among others. Bearing capacity analysis on bimsoils, however, remains limited, with only a few examples available (Campos-Muñoz et al., 2018; Schmüdderich et al., 2021).

In probabilistic studies, the effects of spatial variability are often compared to homogeneous models. However, most comparisons rely on traditional homogenization techniques such as arithmetic or harmonic averages, which generally fail to consider the effects of heterogeneous counterparts. Therefore, probabilistic analyses are necessary. While significant progress has been made in numerical optimization and random field generation, accurate homogenization techniques can provide valuable insights into the behavior of heterogeneous deposits from an engineering perspective. Studies on the random heterogeneity of soil properties assert that phenomena governed by highly non-linear constitutive laws are affected the most. Nobahar and Popescu (2000), Griffiths and Fenton (2001), Li et al. (2015) Popescu et al. (2005a), among others, have studied the effects of inherent random soil heterogeneity on the bearing capacity (q_u) of shallow foundations. All of them have used Monte Carlo Simulation (MCS) considering a continuous heterogeneous field. However, bimsoils consist of two very different soil types hence spatial variability effects could be better understood if binary random fields are considered. These fields have already been utilized to analyze the effects of settlement on structures founded on improved liquefiable soils by Montoya-Noguera and Lopez-Caballero (2016).

This paper presents a comprehensive comparative study of homogenization techniques for evaluating the bearing capacity of bimsoils under shallow foundations. The study specifically examines three aspects: (1) the effect of the spatial fraction of the blocks, (2) the influence of isotropic and anisotropic spatial correlations, and (3) the impact of the contrast on the block and the matrix mechanical properties. These aspects are crucial in understanding the behavior of bimsoils and their implications for geotechnical design. By considering different block arrangements, sizes, and mechanical properties, the study provides insights into the effects of spatial variation on the bearing capacity of shallow foundations. Furthermore, the investigation explores the use of different homogenization theories to account for the average effects of spatial variation.

2. Models and Theories

This section presents first the model for generating binary random fields to simulate bimsoils, followed by the different homogenisation theories used in this paper. Finally the numerical model for the assessment of bearing capacity is shown.

2.1. Binary random field (BRF)

The binary random field (BRF) is generated with the homogeneous autologistic model derived by Bartlett and Besag (1969). It is a nearest-neighbor model defined as a conditional probability, instead of a joint probability distribution as done with the Gaussian Markov random field models (Whittle, 1963). That means it treats dependence directly through the so-called *autocovariate*, which is a function of the observations themselves. The one-sided approximation of the conditional autoregressive binary model in two dimensions under the assumption of homogeneity was derived from the Ising model to a 1st order Markov serie by Honjo (1985). The assumption of homogeneity implies that the underlying spatial process is stationary, meaning that the probability of a material being at a particular location is constant across the entire study area. According to Hughes et al. (2011), this model is straightforward to implement and fast to compute as the probability of a material at a specific location depends on the presence or absence of the material in only two nearest neighboring locations. The model will be briefly discussed; however, more information can be found in Bartlett and Besag (1969); Besag (1972); Honjo (1985) and Montoya-Noguera and Lopez-Caballero (2016).

The binary mixture used to model the heterogeneous zone is defined by three parameters: the spatial fraction (γ) and the auto-regressive coefficients in the horizontal and vertical directions, respectively (β_H and β_V). Under the condition of homogeneity, γ is equal to the expectation of x_{ij}, a value of the binary random variable X_{ij} where i and j denote the position in the horizontal and vertical direction, respectively, in a 2D coordinate system. Following the one-sided approximation, this expectation is given by:

$$E[x_{ij}|x_{i-1,j}, x_{i,j-1}] = \left[1 - \frac{1}{2}(\beta_H + \beta_V)\right] \cdot \gamma + \frac{1}{2}\left(\beta_H \cdot x_{i-1,j} + \beta_V \cdot x_{i,j-1}\right) \quad (1)$$

Thus, the probability of which material is in the position (i, j) depends on the nearest-neighboring binary variables $x_{i-1,j}$ (left neighbor) and $x_{i,j-1}$ (upper neighbor). This one-sided approximation approach assumes that the conditional probabilities depend only on the states of two neighboring variables, not on the states of the variables in the opposite direction. This allows for a more tractable computation of the expectation. Which makes the model easy and quick to compute. The spatial fraction is defined as the areal ratio of blocks with respect to the total area, i.e. $\gamma = N_{blocks}/(N_{blocks} + N_{matrix})$ where N_m is the number of elements of material m. Thus, a γ value of 0 indicates a pure

matrix soil while a value of 1 indicates only blocks. For engineering applications, γ is related to the areal block proportion in two dimensions; hence, it can be calculated from the sum of the areas occupied by blocks with respect to the total area. Napoli et al. (2020) showed that the areal block proportions may vary significantly for a given volume of bimsoil under analysis. However, since a 2D analysis is carried out for the practical application, the spatial fraction will be used herein.

Because of the simple derivation of the autocorrelation function (ρ). Honjo (1985) stated that the one-sided approximation is preferred to the general case. Thus, ρ is equal to $\beta_H^i \cdot \beta_V^j$, where β_H and β_V have a direct physical interpretation as they give the one-step correlation of the process in the horizontal and vertical direction, respectively. Note that the auto-regressive coefficients are dimensionless, as they depend on the spatial discretization, i.e. the total size of the finite element model divided by the number of elements. Figure 1 shows ρ for different β values with β_H equal to β_V. Note that the correlation structure shows an exponential decay, which is expected as it was assumed the Markov definition of order 1.

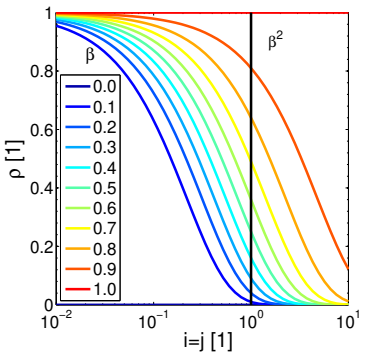

Figure 1: Autocorrelation function (ρ) for different isotropic correlations (β_H=β_V).

For each element, the generated probability is not a binary number, so it is compared to a random number (u_{ij}) that follows a uniform distribution function between 0 and 1, where each element is independent. This process, known as binarization, makes use of MCS to converge to a given γ value, thus preserving the underlying probability without being too sensitive to outliers. This model offers valuable insights into spatial dependence and binary outcomes, however it has some limitations. Due to the one-sided approximation, the model is sensitive to boundary effects thus the obtained spatial fraction may differ from the target one. Honjo (1985) stated that this limitation is negligible if the size of the model is large enough. To avoid this, a tolerance error was set to 1% between the target and the obtained spatial fraction. In addition, as β_H and β_V define an exponential correlation structure, the field is highly sensitive even for lower values (as shown in Figure 1 (Honjo, 1985). In this regard, the number of simulations required to achieve convergence will be higher for higher correlations

and for anisotropy. This aspect will be evaluated in the next section.

Contrary to other algorithms used for modeling bimsoils (e.g. Suarez-Burgoa et al. (2019) and Schmüdderich et al. (2021), the blocks do not have circular shapes. Due to the spatial correlation, the bimsoils generated correspond to polydisperse 2D block distributions where the block sizes are nonuniform. In bimsoils not only the block area proportion (spatial fraction) but also the size distribution plays an important role. When the isotropic correlation increases, the binary soil tends to show a more concentrated spatial distribution in clusters. The mean equivalent block size ratio (BSR_{eq}) was evaluated for the different isotropic correlations and the different spatial fractions and the results are shown in Figure 2. As defined by Schmüdderich et al. (2021), the BSR value is the ratio between the block diameter and the footing width for a monodisperse distribution of spherical blocks. However, as the model generates nonuniform blocks, the equivalent diameter was obtained by clustering analysis using the code for connected components in binary image from the Image Processing Toolbox in Matlab named bwconncomp. Then, the mean value of all clusters for 100 distributions was determined. The results range from 0.08 to 0.2 for a γ value of 0.1 and increases to 0.3 for γ=0.5, where the BSR_{eq} value increases with the spatial correlation. But, for γ values above 0.5, the size of the block clusters increases exponentially and is higher for lower spatial correlations. For instance, for γ=0.9, the BSR_{eq} value is 1.76 for β_H=β_V=0.9 and 3.35 for β_H=β_V=0.1.

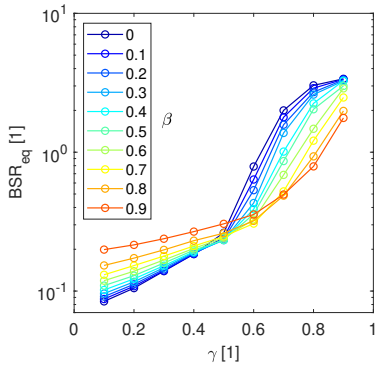

Figure 2: Equivalent block size ratio (BSR_{eq}) for different isotropic correlations (β_H=β_V).

Lastly, the BRF model simulates only welded bimsoils, thus no difference in strength is assumed for the interface between the matrix and the blocks. Napoli et al. (2022) avoided the classification between welded and unwelded bimrocks, used for example by Sonmez et al. (2009), as it can be extremely difficult to estimate the interface strength. However, Schmüdderich et al. (2021) evaluated numerically this effect on the bearing capacity and found lower results for unwelded bimsoils, compared to welded ones, because the lower strength at the interface conditions the failure surface to pass through these weaker areas. For welded bimsoils, the failure surface is only conditioned by the location of the blocks for a given γ value. Hence more variability will be expected for γ

values near 0.5. This aspect will be explored in the next section.

2.2. Homogenisation theories

Traditional homogenisation theories are often used to describe geotechnical properties. For example, the work on spatial variability effect on bearing capacity of Popescu et al. (2005a) often compares the average results of the heterogeneous soil models with the "corresponding homogeneous soil". According to the authors, the homogenisation is the mean value of the Monte Carlo simulations; although this is only true for vertically layered materials (i.e. parallel to the bearing capacity) described by classical homogenisation theories. If, on the contrary, the layers are horizontal (i.e perpendicular or serial) the effective properties of the homogeneous model would be a harmonic average. It is clear that for random fields, these are only extreme cases which are known as Wiener (1912) bounds. The bearing capacity (q_u) of the equivalent homogeneous model will be described as:

- Parallel (arithmetic average) :

$$q_{u\,||} = (1-\gamma)\cdot q_{u\,matrix} + \gamma \cdot q_{u\,block} \tag{2}$$

- Serial (harmonic average):

$$q_{u\,\perp} = \frac{1}{\frac{(1-\gamma)}{q_{u\,matrix}} + \frac{\gamma}{q_{u\,block}}} \tag{3}$$

where $q_{u\,matrix}$ and $q_{u\,block}$ are the bearing capacity values for a pure matrix soil (i.e. when the spatial fraction γ=0) or a pure block soil (i.e. γ=1), respectively. Among the common types of averages, there is also the geometric average, which lies between the arithmetic and harmonic ones. It favours low values, although not as drastically as does a harmonic average. Griffiths and Fenton (2001) evaluated these averages for a lognormally distributed random field of soil strength over a domain of about the size of the plastically deformed bearing failure region. According to these authors, the geometric average showed the best agreement. However, an empirical adjustment for the mean value was used in the Prandtl's formula.

Another case that can be exactly modelled as homogeneous consists of concentric-shell structures, i.e. one material coating the other like spheres of different size. In this case, the properties can be described by the Hashin and Shtrikman (1962) equation:

$$q_{u\,HS^{+}} = q_{u\,block} + \frac{1-\gamma}{\frac{1}{q_{u\,matrix}-q_{u\,block}} + \frac{\gamma}{d\cdot q_{u\,block}}} \tag{4}$$

$$q_{u\,HS^{-}} = q_{u\,matrix} + \frac{\gamma}{\frac{1}{q_{u\,block}-q_{u\,matrix}} + \frac{1-\gamma}{d\cdot q_{u\,matrix}}} \tag{5}$$

where d is the dimensionality. This parameter binds the model to fluctuate between the Wiener bounds; hence, when d is equal to unity, they become the parallel bound and as it tends to infinity they approach the perpendicular one. Actually, HS bounds are narrower than the Wiener bounds and are often used as they are simple and intuitive. However, they still give wide predictions, specially if the ratio between the material properties is big.

Besides these traditional homogenisation theories, another approach consists in identifying an effective property -in this case $q_{u\,eff}$- for which the average behaviour of the heterogeneous model remains unchanged. Among them, probably the most common is the Bruggeman (1935) effective medium (BEM) equation, which is a classical theory of conduction in mixtures also known as the symmetric effective medium approximation. When the properties of both materials are of similar magnitude, the BEM equation is:

$$(1-\gamma)\frac{q_{u\,matrix}-q_{u\,eff}}{q_{u\,matrix}+(d_{BEM}-1)\cdot q_{u\,eff}}+\gamma\frac{q_{u\,block}-q_{u\,eff}}{q_{u\,block}+(d_{BEM}-1)\cdot q_{u\,eff}}=0 \quad (6)$$

where d_{BEM} is equal to half the mean number of bonds presented at any site of the network (Kirkpatrick, 1973). The BEM equation gives a more precise solution as it accounts for each material independently. An important aspect of this equation is the adaptability of the d_{BEM} parameter for each bimsoil. Thus, contrary to the geometric average recommended by Fenton and Griffiths (2002), the BEM equation can be fitted to different bimsoils as will be seen later on.

2.3. Numerical model

A finite element model (FEM) is used to evaluate the bearing capacity of a shallow foundation. Two-dimensional plane-strain analyzes are performed with the general purpose finite element code GEFDyn (Aubry and Modaressi, 1996). The numerical model uses quadrilateral isoparametric elements with eight nodes. A rigid perfectly plastic model is implemented to simulate the behavior of purely cohesive soils. While the Young modulus (E) and the Poisson's ratio (ν) influence the computed settlement, the bearing capacity of a footing depends primarily on the undrained shear strength (c_u) (Griffiths et al., 2002). Thus in the present study, to simplify the analyses, E and ν are kept constant and equal to 100MPa and 0.3, respectively. Each simulation of the binary random field is used as input for c_u at each element on the model. Hence, for binary value (x_{ij}) equal to 0, the matrix is used with, initially, $c_{u\,matrix}$ equal to 20kPa; and for x_{ij}=1, block is used with $c_{u\,block}$ = 100 kPa.

Bimsoils are characterized by discrete blocks within a finer-grained matrix. As stated by Medley and Zekkos (2011), the term "geotechnically significant blocks" means that there is a mechanical contrast between blocks and matrix that forces a tortuous failure surface around the blocks. Limiting values to define that mechanical contrast are given for types of failure and different parameters as shown in Table 1. The authors also state that relatively modest block-matrix mechanical contrast is necessary for a block-in-matrix mass to be considered.

Failure	Criterion	Value
Triaxially induced shears	E_{block}/E_{matrix}	≥ 2.0
Deflect failure surfaces	$\tan\phi_{block}/\tan\phi_{matrix}$	≥ 1.5 - 2.0
Unconfined Compressive Strength	UCS_{block}/UCS_{matrix}	≥ 1.5

Table 1: Block-matrix strength contrast using estimates of weakest block and matrix mechanical parameters (Medley and Zekkos, 2011; Kalender et al., 2014)

Below these values, the failure surface would have an increased tendency to pass through the blocks rather than around them. If the bearing capacity is assumed to be controlled by the failure on undrained conditions, i.e. the loading rate of the foundation's construction is higher than the pore water pressure dissipation, the c_u value is equal to half the Unconfined Compressive Strength (UCS). Results will be presented first for a strength contrast of 5 and in section 4.3 lower and higher contrast ratios will be tested.

A schema of the model is shown in Figure 3. The dimensions are given by the width of the base (B), in this case 4m, and are taken from the recommendations of Griffiths and Fenton (2001): a depth of 2B (8m) and a width of 5B (20m). The size of the elements is 0.25 m in both directions which corresponds to B/16, which was also used by Chen et al. (2012). A rigid bedrock underlies the soil hence no vertical displacements are allowed on the bottom of the model and as only vertical loads are applied, horizontal displacements are inhibited on the lateral boundaries, as shown by equations 7 and 8.

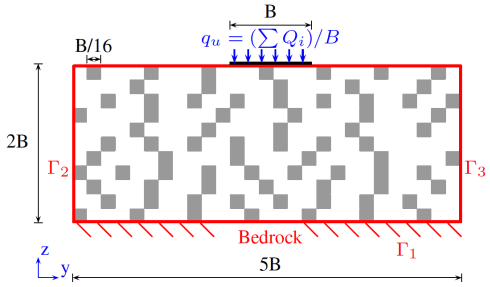

$$\underline{u} \cdot e_y = 0 \quad \forall \underline{x} \in (\Gamma_1 \cup \Gamma_2 \cup \Gamma_3) \tag{7}$$

$$\underline{u} \cdot e_z = 0 \quad \forall \underline{x} \in \Gamma_1 \tag{8}$$

Figure 3: Schema of the numerical model

The test consists of applying an increasing vertical displacement (u_z) at the center of the foundation (i.e. at one node) with free rotations allowed for the foundation. As the latter is rigid, a uniform displacement is considered in this interface. The ultimate bearing capacity is taken when $u_z/B = 2.5\%$ (10 cm) and is equal to the sum of the nodal forces (Q_i) in the interface between the soil and the structure's foundation divided by the width of the base (i.e. $q_u = (\sum Q_i)/B$).

For a homogeneous weightless soil, the bearing capacity is given by the Prandtl's solution as $q_u = N_c \cdot c_u$, where N_c is the dimensionless bearing capacity

factor and equals $2 + \pi$ or 5.14 (Prandtl, 1921). The finite element analysis of the homogeneous cases, specifically when considering only the matrix or only the blocks, revealed a relative difference of 6.85% and 14.7%, respectively, in comparison to Prandtl's solution. The former is one percentual point lower than the results of Chen et al. (2012) with the same properties and mesh size and similar to those of Popescu et al. (2005b). These differences are due to the assumptions in the model, for example, concentration of shear stresses at the soil-structure interface, gradual development of plastic zones, as well as inherent approximations induced by the numerical methods which are further explained by Nobahar (2003).

Furthermore, the difference with respect to Prandtl's solution depends on the mesh size. Refining the mesh can assist in reducing these differences, albeit they cannot be entirely eliminated. However, this refinement comes at the expense of increased computational resources needed for the subsequent random-field simulations. Other researchers have evaluated the impact of increasing mesh discretization, i.e., the number of elements in each direction. For instance, Chen et al. (2012) demonstrated an approximately 50% decrease in numerical error when the mesh discretization was increased by a factor of 4.

Another factor of mesh discretization in the accuracy of predicting q_u, is capturing the concentration of plastic strain within narrower zones. As the footing is assumed rigid, the vertical stress distribution is non-uniform and stress concentrates near the edges of the footing, resulting in higher plastic strains. However, considering this effect would introduce additional complexity to the generation of the random field, which is beyond the scope of this study. Considering the extensive number of random field simulations performed, the chosen mesh size was deemed both efficient and suitable for the purposes of this study.

3. Coupling the binary random field with FEM

The spatial discretization is used to analyse the heterogeneous deposit. The spatial fraction (γ) is varied from 0.1 to 0.9 (9 values) and 50 spatial distributions per value were done. Different auto-regressive coefficients on both directions were tested to analyse the effect of the correlation length.

As an example, the deformed mesh at failure of two spatial distributions for the same spatial fraction ($\gamma = 0.5$) and the same auto-regressive coefficients ($\beta_H = \beta_V = 0.9$) are shown in Figure 4. The deformation is scaled by a factor of 100 to improve visualization. They correspond to the extreme values of bearing capacity found for this set of values: the minimum shown in Figure 4a (q_u=148 kPa) and the maximum, in Figure 4b (q_u=287 kPa). The soil matrix, which has a smaller c_u, is in red color and the blocks are in blue. Similar to the results of Fenton and Griffiths (2002); Schmüdderich et al. (2021), the failure surfaces are certainly not symmetric and only approximately follow a log-spiral on different sides. It is clear that for the mesh that presented the minimum q_u the soil matrix is mostly concentrated near the foundation which has triggered a non-symmetric failure mechanism; while for the other one, the

blocks under the foundation interconnect from the surface to the deeper zone. The spatial variability is not simply affecting the value of the bearing capacity but it modifies the basic form of the failure mechanism. These two distributions presented very different q_u value, thus a convergence analysis was performed to choose the sufficient number of simulations per γ value.

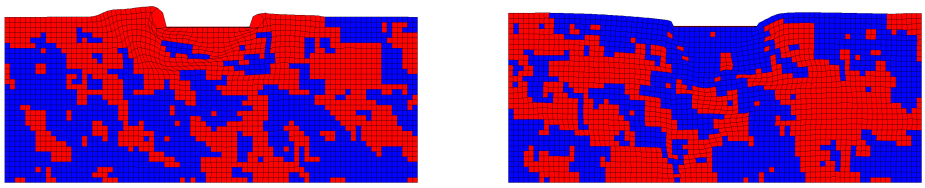

(a) (b)

Figure 4: Deformed mesh at failure for two distribution of bimsoils with $\gamma = 0.5$ and $\beta_H = \beta_V = 0.9$: a) minimum q_u (148 kPa) and b) maximum q_u (287 kPa). The matrix is depicted in red ($c_{u\,matrix}$=20kPa) and the blocks in blue ($c_{u\,block}$=100kPa). The deformation is scaled by a factor of 100.

The convergence of both the mean and the standard deviation of the bearing capacity is shown for one case ($\gamma = 0.7$ and $\beta_H = \beta_V = 0.9$) in Figure 5. The average values are shown in red and the confidence intervals, in dotted blue lines. The latter are obtained with the t-student and χ^2 statistical models with 5% confidence level for the mean and standard deviation, respectively. 200 spatial distributions were tested; although, after approximately 50 the statistical convergence appears to be stable hence is sufficient for the application considered in this work. As expected the mean value converges more easily and presents less variation than the standard deviation. In contrast, the standard deviation has more variation and wider confidence intervals. Here on, a maximum of 50 simulations are performed for each case.

3.1. Effect of the spatial fraction of blocks

The evolution of q_u as a function of γ is shown in Figure 6 for different correlation values. For the sake of brevity only four cases are presented: the uncorrelated model (i.e. $\beta_H = \beta_V = 0$) and 3 other values of isotropic correlation. The box-and-whiskers plot is useful to show scalar-value statistics because of the large amount of uncertainty information compared to mean and standard deviations. Additionally, due to its flattened shape, box plots are better when it is desired to compare the uncertainties in a number of related variables (Helton et al., 2006). The box is composed of 3 quartiles, corresponding to 25, 50 and 75% of data and the whiskers are the lowest and highest values within 1.5IQR (Inter-quartile range). Values outside the whiskers are outliers and are drawn as blue dots. The mean values are in red and joined by the curve.

It is seen in Figure 6a that when no correlation is used less dispersion is presented. Whereas, when a high correlation is used, like shown in Figure

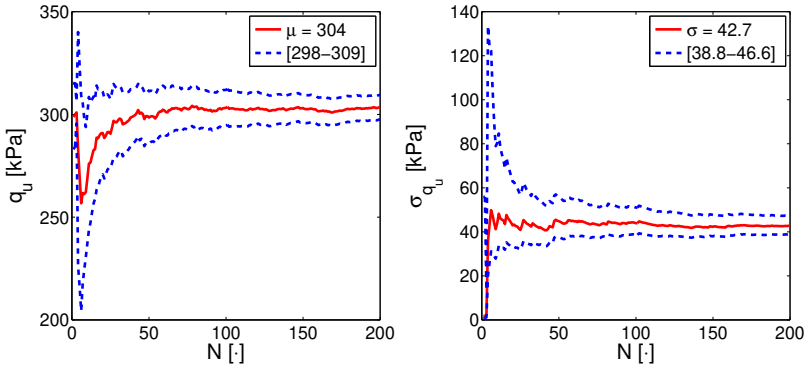

(a) (b)

Figure 5: Convergence of the a) mean and b) standard deviation of the bearing capacity (q_u) for $\gamma = 0.7$ and $\beta_H = \beta_V = 0.9$. The average values are shown in red and the confidence intervals, in dotted blue lines.

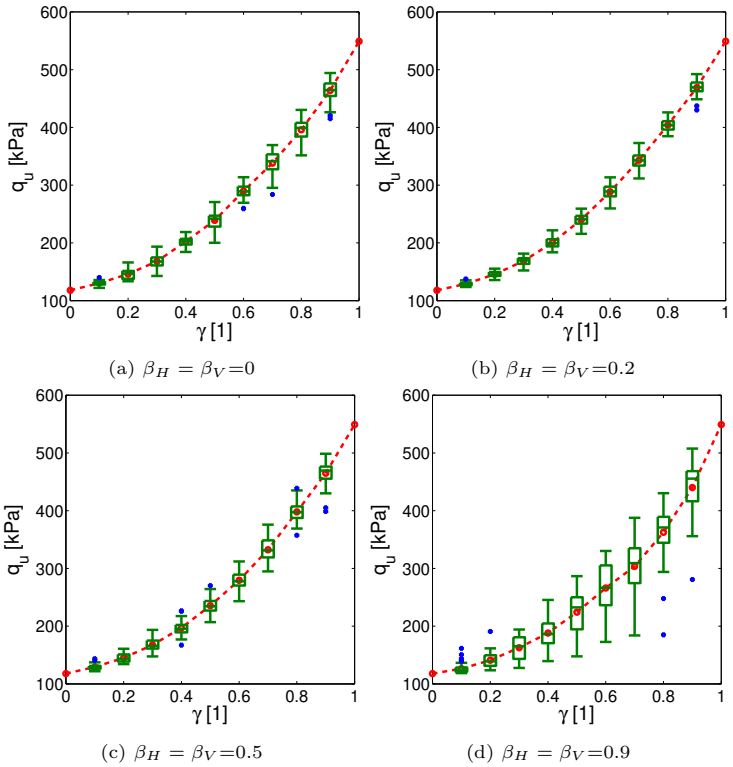

(a) $\beta_H = \beta_V$=0 (b) $\beta_H = \beta_V$=0.2

(c) $\beta_H = \beta_V$=0.5 (d) $\beta_H = \beta_V$=0.9

Figure 6: Models with different spatial fraction γ and different isotropic correlations

6d, the dispersion increases. Additionally, the dispersion is higher for spatial fractions around 0.5; though, it seems that the spatial configuration is of key importance when a similar fraction of both materials is used. This could be explained by the higher interaction between the mixture and the blocks and the resulting failure surfaces. When the isotropic correlation increases, the soils are "packed" in clusters and therefore each distribution will have a different behaviour.

The dispersion in mechanical properties is commonly quantified by the coefficient of variation (CV) and defined as the ratio between the standard deviation and the mean value. Thus, CV is a normalized quantity and it is of great use in probabilistic analysis. Representative values of CV can be found in the literature based on laboratory data, *in-situ* tests or engineering judgement (Phoon and Kulhawy, 1999). Typical CV values are around 10 to almost 60 % for site-specific undrained shear strength in clays and below 40 % for normalized strength (i.e. divided by the vertical effective stress) (ISSMGE-TC304, 2021). In this analysis, the CV of the bearing capacity (q_u), due to discrete spatial variability was calculated for the different spatial fractions and isotropic correlations.

Figure 7 shows the CV value as a function of the spatial fraction for each correlation and for all the distributions tested. It is interesting to note how CV increases with the degree of correlation and it is more important for spatial fractions near 0.5. In general, compared to the ranges given by ISSMGE-TC304 (2021), the values are very low (i.e. below 20%). This is due to the fact that the variability measured is only induced by the spatial variability, referred by other authors as inherent random heterogeneity, and it does not take into account the measurement errors and uncertainty in physical parameters, present in experimental data (Wang et al., 2016). According to these values, thus, it seems that uncertainties due to spatial variability are lower to those related to the strength values (induced by measurement, statistical and transformation errors). Note that the compared ranges are for material properties and the one calculated is for the structure response. However, as for this case the relation between the initial property (i.e. c_u) and the response (q_u) is only a constant value, this comparison is still valid.

3.2. Effect of anisotropic correlation

An important effort is evidenced in geotechnical engineering in order to quantify the correlation length in the spatial variability. Jones et al. (2002) and more recently ISSMGE-TC304 (2021) present a literature review of the scale of fluctuation in horizontal and vertical direction mostly from *in-situ* tests, however the amount of information concerning these values is limited in comparison to the CV of inherent variability. In general, the correlation length in the horizontal direction is between 10 and 20 times larger than in the vertical one. The degree of anisotropy in bimsoils is influenced by various factors, including the processes involved in their formation, as well as the superposition and interaction of these processes (Napoli et al., 2022). At the moment, very little information can be found hence a parametric analysis was performed for different correlations. For

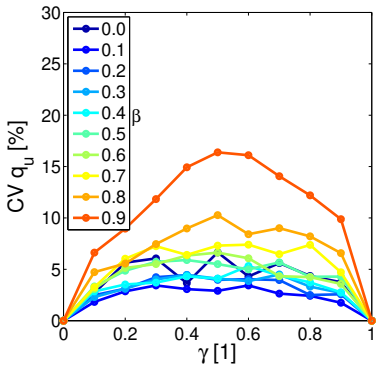

Figure 7: Coefficient of variation (CV) of the bearing capacity (q_u) in bimsoils as a function of the spatial fraction (γ) for different isotropic correlations

a spatial fraction of 0.4, only one correlation was changed from 0.1 to 0.9 while the other one was fixed and equal to 0.1. The mean and CV of the bearing capacity are shown in Figure 8. It appears that the anisotropic correlation is inversely related to the mean and directly related to the CV results. However, the effect of the correlation is more important for the CV value (e.g. for $\beta = 1$, CV is twice the one without correlation; while the decrease in the mean value is only 2%). For this case, the vertical correlation presents in general higher values for both mean and CV. For the sake of brevity, the results are only shown for one spatial fraction, nevertheless other values were tested and they presented the same trends.

4. Homogeneous equivalent models

Homogeneous equivalent models and their effective properties are interesting from an engineering point of view. With the aid of widely used computer software such as Microsoft Excel, performing Monte Carlo Simulation (MCS)-based probabilistic analysis for geotechnical applications is becoming more convenient and straight-forward (Wang and Huang, 2012; Wang et al., 2016). Is it possible to obtain the same probability density functions (PDF) of the bearing capacity using binary random fields (BRF) and homogeneous MCS?

4.1. Monte-Carlo simulations

To develop the homogeneous equivalent model, three steps are performed. A flowchart of this procedure is shown in Figure 9. First, the results from the BRF analysis are used to generate the empirical cumulative density function (CDF) of the bearing capacity (q_u). Second, the CDF of the effective strength ($c_u^{eff}(\gamma)$ is linearly calculated from the previous results considering the Prandtl solution. The third step consists of using the obtained CDF of c_u^{eff} to generate multiple homogeneous fields with Monte Carlo simulations and evaluate the

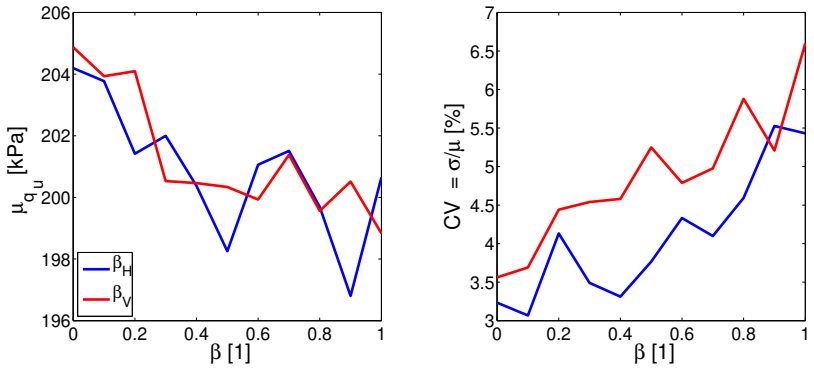

(a) (b)

Figure 8: Anisotropic correlation effect on the a) mean and b) CV of the bearing capacity for bimsoils with a spatial fraction of 0.4. The coefficient in the horizontal (β_H) or vertical (β_V) correlation is varied while the other correlation is fixed to 0.1.

resulting statistical properties of the bearing capacity. Hence, addressing the question regarding the feasibility of achieving identical mean and dispersion using homogeneous models that can faithfully replicate the effect of the spatial variability on the bearing capacity observed in bimsoils. The procedure is shown in detail for different spatial fractions and isotropic correlations.

4.1.1. CDF of the bearing capacity from BRF results

First, the results from the spatial variability simulated with BRF are used to calculate the empirical CDF. Figure 10 shows the normalized CDF of the bearing capacity for γ of 0.1, 0.5 and 0.9 and all different correlations. As it is seen once more, the isotropic correlation plays an important role in the CV (refer to the steepness in the CDF in figures 10b and 10c). Additionally, for γ of 0.9, the type of the distribution changes; though, for instance, the results for β of 0.9 have a lognormal distribution -as it presents a positive skewness- while for β of 0.1, a normal distribution could be more adequate.

Jones et al. (2002) summarized the inherent variability on strength characteristics given by *in-situ* and laboratory measurements and suggest a lognormal PDF for undrained shear strength (c_u) in clays and a normal one for c_u in silty-clays. Hence, as the c_u decreases, the distribution shifts from lognormal to normal, as it does with the results for γ of 0.9. An accurate probability function could be very useful to construct fragility curves that take into account the spatial variability uncertainty in bimsoils. However the success of this kind of analysis requires an accurate safety limit or threshold related to the deterministic properties. In the next section, an effort to find an homogeneous equivalent model will be presented.

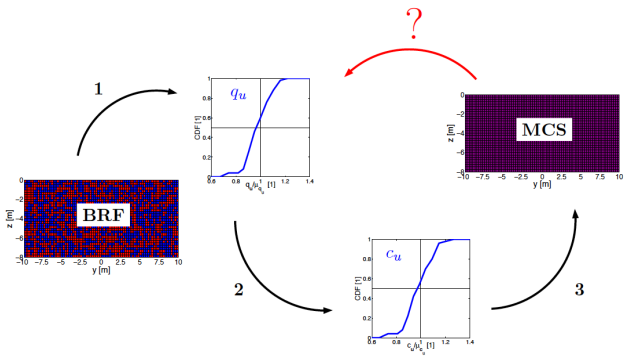

Figure 9: Flowchart of the procedure to generate the homogeneous equivalent model with the same probability distribution

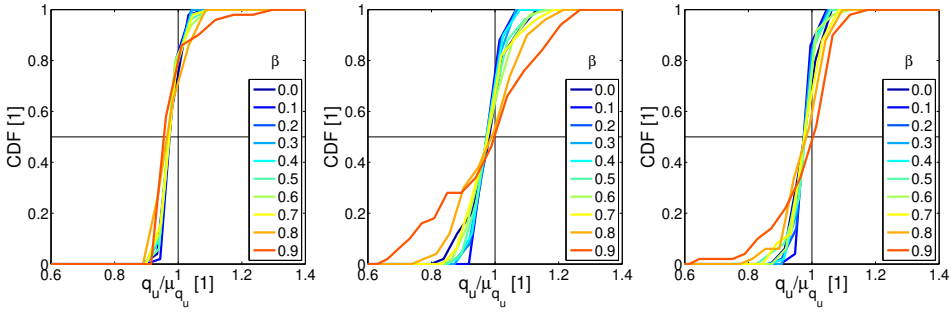

(a) (b) (c)

Figure 10: Experimental cumulative density function (CDF) of the bearing capacity for : a) γ=0.1, b) γ=0.5 and c) γ=0.9

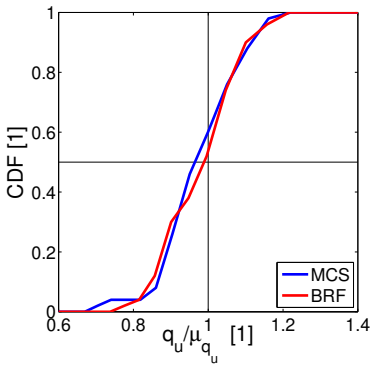

Figure 11: Comparison of the normalized CDF of q_u obtained from the homogeneous Monte Carlo simulations (MCS) and the one obtained from the initial binary random field (BRF) for γ of 0.5 and β_H and β_V equal to 0.8

4.1.2. CDF of the equivalent undrained shear strength for homogeneous models

Second, as q_u depends only on the undrained shear strength, the effective property (c_u^{eff}) is equal to $\mu_{q_u}(\gamma)/5.14$, where μ, indicates the mean value of all the q_u values resulting of the spatially variable models for a specified γ. It is reasonable to believe that the same numerical error - i.e. 10% in average - with respect to the Prandtl solution is present in all cases; therefore, for the homogeneous model the error is deducted from the effective property (otherwise it would be counted twice). Thus, the resulting CDF of q_u from the first step is divided by 5.14 and corrected due to numerical errors to obtain the CDF for c_u^{eff} that will be used as input in the next step.

4.1.3. CDF of the bearing capacity from homogeneous MCS

Monte Carlo simulations involve generating a large number of random samples from a known probability distribution to approximate various statistical properties of a system. In this context, the CDF of the c_u^{eff} is used to simulate 200 homogeneous fields. The results of the MCS are used to obtain the CDF of q_u. Figure 11 compares the empirical CDF of q_u from the BRF models (step 1) and from the homogeneous MCS (step 3). For the sake of brevity, results are only shown for one set of spatial fraction and correlations. It corresponds to γ of 0.5 and β_H and β_V equal to 0.8. The resulting CDF from the MCS matches very well the one from the BRF analysis. Hence the effect of spatial variability can be included in homogeneous analysis with the use of probability functions. Now, the question relies on how to describe such function in a general case according to the soil parameters.

4.2. Homogenisation theories

In engineering practice, it is common to use deterministic homogenisation theories to simplify the average effects of spatial variation. Figure 12a shows

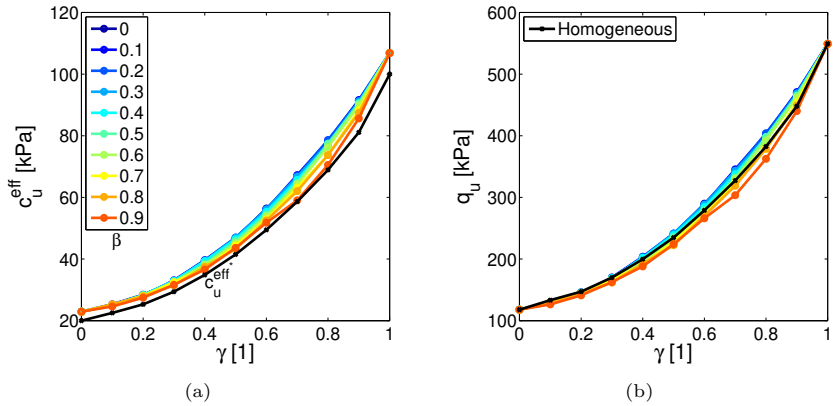

Figure 12: Input and Output of the homogeneous equivalent model : a) Effective property ($c_u^{eff} = \mu_{q_u}(\gamma)/5.14$) for all isotropic correlations and average corrected value ($c_u^{eff^*}$), in black, used as input and resulting b) Bearing capacity q_u as a function of the spatial fraction (γ) in black compared to the average of the heterogeneous models

the mean of c_u^{eff} as a function of γ for all the different correlations. As in the previous analysis, the undrained shear strength is corrected from the FE error. The average corrected effective property ($c_u^{eff^*}$), shown in the figure in black, was used for the deterministic homogeneous equivalent model. In Figure 12b, the results are compared with the q_u mean values of all the correlations. As expected, the homogeneous models have the same behaviour and could be described by an equation. It is important to note that the homogeneous model takes into account all the correlations tested and their respective dispersion; however the general behaviour with respect to the spatial fraction (i.e. the shape of the function) is the same for all cases hence the equation should be similar.

The traditional homogenisation theories are compared to the numerical results in Figure 13a. It shows the mean q_u values normalized by the $q_{u\,block}$ as a function of γ and the Wiener and HS bounds. As it is shown, if the homogeneous models take the upper Wiener bound described by the arithmetic average (i.e. diagonal straight line in Figure 13a) as the effective property, the heterogeneous model will always present lower resistance (i.e. lower q_u values). Overall, results are inside the HS bounds with a d value of 2. However, for lower spatial fractions ($\gamma < 0.4$) the mean values are even lower than the HS^- bound and almost similar to the lower Wiener bound described by the harmonic average. Nonetheless, this harmonic average is significantly lower than the numerical results for higher γ values.

In contrast, as it can be seen in Figure 13b, the mean values are well fitted by the BEM equation in which, for the case tested, d_{BEM} was found by a root-mean-square fit to a value of 1.5. Though if an homogeneous equivalent model should be compared with discrete spatial heterogeneous models, BEM should

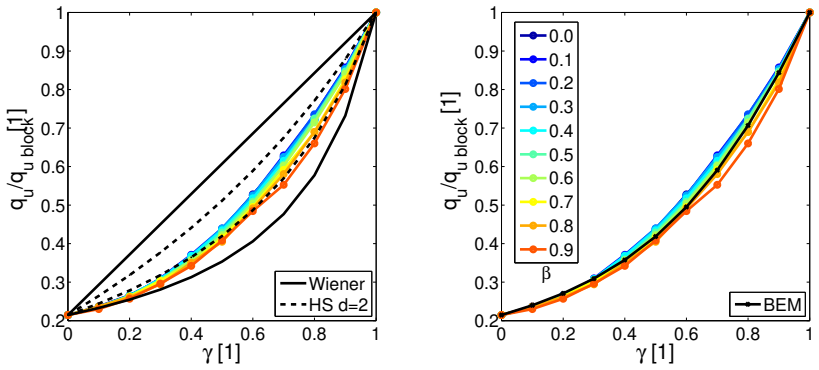

(a) (b)

Figure 13: Heterogeneous mean normalized q_u values compared to a) traditional homogenisation and b) Bruggeman symmetric effective medium theories ($d_{BEM} = 1.5$)

be used.

4.3. Effect of the contrast in the matrix and block properties

The spatial variability effect depends on the matrix and block soil properties; hence, seven more strength ratios ($c_{u\,block}/c_{u\,matrix}$) were used and the normalized mean and CV values are shown in Figure 14. No correlation was introduced, which was found to increase the variability, and its effects have been formerly addressed. The undrained shear strength (c_u) of each set and the respective ratios are shown in Table 2. In Figure 14a, the lower and upper quartiles (i.e. 25 and 75%) are also shown however the dispersion is very low compared to the mean value. Note that as the ratio increases, the shape of the model changes thus it could only be represented by an equation with an additional parameter, such as the d_{BEM} of equation 6. Moreover, for the last two cases, where the ratios are repeated but with different c_u values, the normalized behavior does not change. Hence, it depends more on the contrast between the materials and not on the values used.

Figure 14b shows the CV values of all the c_u ratios tested. In general, as the contrast between the block and matrix strength increases, there is a corresponding increase in dispersion, akin to what is observed with higher levels of isotropic correlation. This phenomenon is expected because a greater difference in strength implies a more pronounced change in the failure surface. Notably, the CV values tend to be higher for spatial fractions near 0.5, with the exception of the two cases with a contrast ratio of 20. The increase in dispersion nearing equal fractions of blocks and matrix might be related to the clustering effect that produces an increase in equivalent block size as shown in Figure 2. As for the cases of a c_u ratio of 20, the largest CV values are observed for spatial fractions of about 0.2 possibly because when the blocks occupy only a small portion of the material, the strength of the matrix dominates the bearing capacity in the

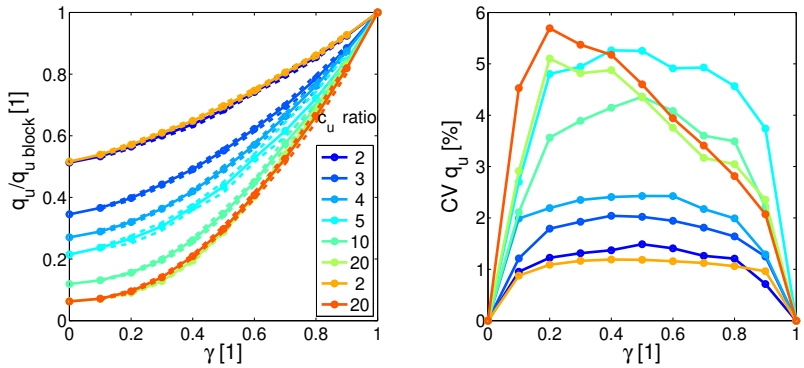

(a) (b)

Figure 14: Different bimsoils c_u ratios tested: a) mean and percentiles 25 and 75% and b) CV values

ratio	$c_{u\,matrix}$ [kPa]	$c_{u\,block}$ [kPa]
2	20	40
3	20	60
4	20	80
5	20	100
10	10	100
20	10	200
2	30	60
20	5	100

Table 2: Sets of parameters tested

model thus inducing more intricate failure surfaces. Nevertheless, it is worth highlighting that for all cases, the CV remains below 6%, which is less than half of the maximum value attributable to isotropic correlation, of almost 16% as depicted in Figure 7.

Finally, the BEM equation was used to fit the bearing capacity of the different sets of soils tested. The parameter d_{BEM} was found by the minimization of the root-mean-square error. The results are shown in Figure 15. It is interesting to note that the changes in the shape of the curves from the bearing capacity ratio as function of the spatial fraction, shown in Figure 15a, for the different c_u ratios, agree very well with the d_{BEM} proposed. Figure 15b shows the relationship between the proposed values for d_{BEM} and the c_u ratio. A power equation appears to fit the data with a R^2=0.99, as following:

$$d_{BEM} = (c_{u\,matrix}/c_{u\,block})^{0.28} \tag{9}$$

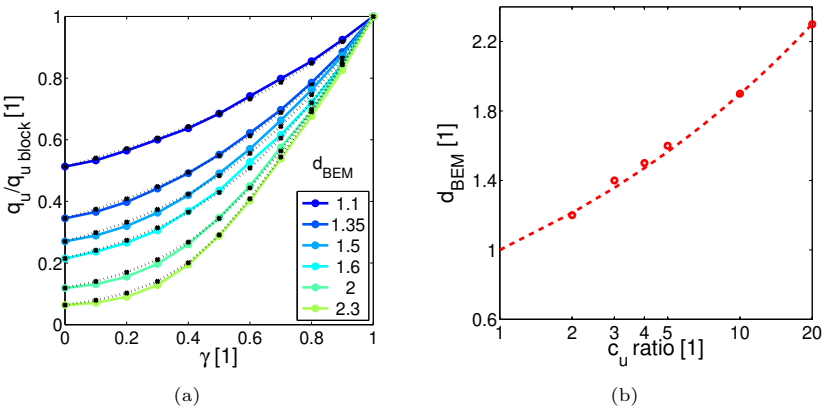

(a) (b)

Figure 15: BEM equation for the different c_u ratios tested: a) bearing capacity ratio as function of the spatial fraction and b) d_{BEM} values as a function of the c_u ratio.

4.4. Effect of the effective loaded zone

As depicted in Figure 4, it becomes evident that not the entire strength of the soil deposit is crucial when evaluating the bearing capacity (q_u) of the foundation. Instead, there appears to be a defined region for which the average shear strength is related the most with the q_u value. The existence of an equivalent homogeneous soil deposit that could reproduce (statistically) the same response as a spatially variable deposit is encouraging for practical purposes. Pioneering work by Vanmarcke (1977) stated that the performance of geotechnical structures is controlled by the average over a certain size of line, area or volume, referred as the Local Average (LA), rather than by the soil parameter value at a single point. In fact, LA is recommended in practical design codes, such as Eurocode 7 (CEN, 2004), to determine characteristic values of geotechnical parameters. LA applications in the assessment of the bearing capacity have been studied by Asaoka and Matsuo (1983), Griffiths and Fenton (2001) , Kasama et al. (2012) and Honjo and Otake (2013), among others. The former proposed appropriate sizes of local averages to evaluate the effects of spatial variability for various geotechnical structures. Concerning the bearing capacity of shallow foundation in cohesive soils, a size of $L_y \times L_z$=$2B \times 0.7B$ was suggested. It corresponds to the rectangle where is located the majority of the plastic zone obtained by the Prandtl-type ultimate bearing capacity equation. This size was said to be independent of the random field characteristics and of the absolute undrained strength of the soils. Thus, the averaging area size purely depends on the mechanism controlling the limit state, but not on the spatial variability properties of the soil.

For the binary random field used to simulate bimsoils presented in this analysis, an optimization procedure was established to find the LA area. For the sake of brevity, only the case of maximum variation is presented, i.e. $\beta_H = \beta_V = 0.9$; however, the other cases were also analysed and the results were similar. The

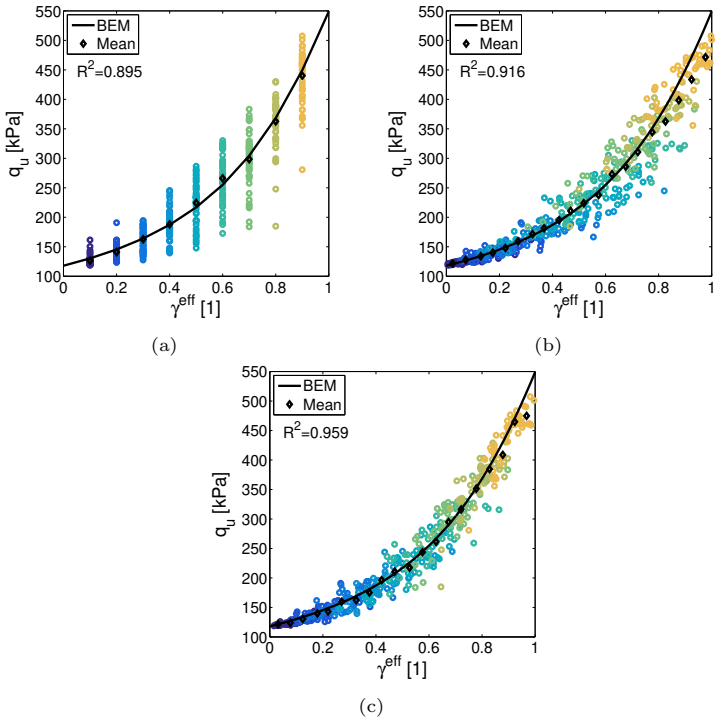

Figure 16: Bearing capacity as a function of the γ^{eff} : a) evaluated in all the deposit ($5B \times 2B$) , b) at the suggested area by Honjo and Otake (2013) ($2B \times 0.7B$) and c) the optimized area ($2.4B \times B$).

optimization consisted in maximizing the coefficient of determination (R^2) of the data fitted to the previously obtained BEM equation. In the fit, the bearing capacity values are related to the effective spatial fraction (γ^{eff}), calculated at the area below the foundation of size $L_y \times L_z$. The distances $L_y/2$ and L_z were varied every element size ($B/16$). As an example, three cases are shown in Figure 16 : a) evaluated in all the deposit ($5B \times 2B$) , b) at the suggested area from Honjo and Otake (2013) ($2B \times 0.7B$) and c) the optimized area found ($2.4B \times 1.1B$). Globally, the dispersion is reduced when using an appropriate γ^{eff}, although some dispersion is still present for the optimized area. Concerning the mean values evaluated at different bins, the BEM equation is in general appropriate for the three cases, except for higher γ^{eff} as shown in Figure 16b.

A summary of the optimization is shown in Figure 17. The R^2 values for each area tested are mapped in the mesh. As the results are vertically symmetric, only half of the mesh is shown. Even if the R^2 value for the area of $2B \times 0.7B$, shown in dashed box, is high ($R^2 = 0.916$), it is improved for the optimized area ($R^2 = 0.959$), as shown in the solid box. The remaining box, in dash-dot, corresponds to the entire plastic zone of the Prandtl-type ulti-

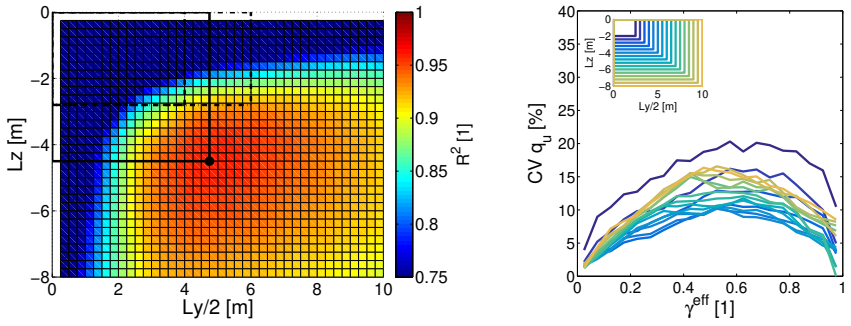

(a) (b)

Figure 17: Optimization summary results: a) Half mesh for the coefficient of determination R^2 values of varying LA area and b) CV reduction due to LA area in bimsoils

mate bearing capacity equation and presented a smaller R^2 value. Figure 17b demonstrates that optimizing the LA area leads to a significant reduction in the coefficient of variation (CV), nearly halving its value. The CV reduction was also evaluated for the other isotropic correlations tested; however it was smaller and is not shown here to avoid repetition. While the CV is reduced when the optimized area is used, there is still a remaining dispersion due to the different failure mechanisms induced by the spatial variability. Compared to the initial CV values, from Figure 7, the maximum value is still higher for this isotropic correlation. In other words, the variation due to the spatial correlation in bimsoils is more important than that of the local average.

5. Conclusions

Homogeneous equivalent models can present the same q_u values when the accurate c_u value of bimsoils is taken as input. Because of its capability to account for the contrast in matrix and block mechanical properties, the Bruggeman effective medium (BEM) equation appears to accurately predict the mean bearing capacity for varying spatial fractions (γ). On the contrary, traditional homogenisation techniques, such as the arithmetic or harmonic averages, will either overestimate or underestimate the resistance of bimsoils. However, for a given γ and a given correlation, the spatial distribution affects the q_u with coefficients of variation (CV) up to almost 20%. This CV can be reduced if the optimized LA area is taken into account, although it can not be avoided as it is due to the radically different failure mechanisms (surfaces) that are developed. Lastly, these variations can be also obtained with Monte Carlo simulations on homogeneous models which could be of great use to account for the effects of bimsoils spatial variability on the bearing capacity in a simple reliability-based design.

The results shown in this analysis have taken into account the results difference with the Prandtl's solution. First, it has been measured as the ability

of the finite element method to reflect the actual behaviour of an homogeneous (ideal) soil and it has been subtracted before applying the Prandtl's formula. It has been assumed that both the finite element method and the theoretical formula are sufficiently reasonable approximations to the behaviour of soils to allow the investigation of the major features of stochastic bimsoils behaviour under loading from a rigid foundation. Note that the effects of the spatial variability in the CV of q_u have been evaluated independently of these assumptions and are associated with traditional usage of this engineering problem.

The numerical model of binary spatial variability applied in a probabilistic framework appears to properly include heterogeneity on the bimsoils. Other cases of discrete spatial variability, such as soil-mixing for liquefaction mitigation, have been also analyzed with this model in order to identify homogeneous equivalent models (Montoya-Noguera and Lopez-Caballero, 2016). Homogeneous equivalent models with the BEM equation were successfully calibrated for eight sets of contrast between matrix and block undrained shear strength values to evaluate the bearing capacity under undrained conditions. For further research, other values for contrast in strength and stiffness properties between the blocks and matrix may be tested evaluating also the settlement and other engineering demand parameters. Also, other constitutive models may be implemented, representing for example a purely frictional matrix as done by Schmüdderich et al. (2021). Additionally, a continuous random field model could be included in order to account for inherent variability in the matrix and the block behavior. Bimsoils were simulated with a binary random field (BRF) model and a uniform mesh was used. Employing adaptively refined meshes such as that presented by Schmüdderich et al. (2021) may bypass the computational resources while at the same time enhancing accuracy by utilizing a smaller total number of elements. This technique is of even greater importance in scenarios where irregularly shaped blocks can impede the development of regular failure surfaces. This could be an improvement for further studies. The BRF model produced polydispersed clusters with irregular shapes of different sizes controlled partly by the correlation coefficients, although the model could be enhanced to produce regular shapes of fixed sizes. Finally, the results presented are limited to welded bimsoils but unwelded bimsoils could be also studied with this numerical model and with adaptively refined meshes.

References

Asaoka, A., Matsuo, M., 1983. A simplified procedure for probability based ϕ_u=0 stability analysis. Soils and Foundations 23, 8–18.

Aubry, D., Modaressi, A., 1996. GEFDyn - manuel scientifique. Ecole Centrale Paris, France: LMSSMat.

Bartlett, M., Besag, J., 1969. Correlation Properties of Some Nearest-Neighbor Models. Bulletin of the International Statistical Institute 43, 191–193.

Besag, J., 1972. Nearest-Neighbour Systems and the Auto-Logistic Model for Binary Data. Journal of the Royal Statistical Society 34, 75–83.

Bruggeman, D.a.G., 1935. Berechnung verschiedener physikalischer Konstanten von heterogenen Substanzen. I. Dielektrizitätskonstanten und Leitfähigkeiten der Mischkörper aus isotropen Substanzen. Annalen der Physik 416, 636–664. doi:10.1002/andp.19354160705.

Campos-Muñoz, D.D., Ramos-Cañón, A.M., Prada-Sarmiento, L.F., 2018. Evaluation of bearing capacity in Bimsoil under a shallow foundation using FEM (en español: Evaluación de la capacidad portante en un Bimsoil bajo una cimentación superficial mediante FEM). Revista Tecnica De La Facultad De Ingenieria Universidad Del Zulia 41, 86–94.

CEN, 2004. Eurocode 7, Geotechnical design. European Committee for Standardization, Brussels, Belgium. EN1997-1 part 1: general rules, seismic actions and rules for buildings.

Chen, Q., Seifried, A., Andrade, J.E., Baker, J.W., 2012. Characterization of random fields and their impact on the mechanics of geosystems at multiple scales. International Journal for Numerical and Analytical Methods in Geomechanics 36, 140–165. doi:10.1002/nag.999.

Fenton, G., Griffiths, D., 2002. Probabilistic foundation settlement on spatially random soil. Journal of Geotechnical and Geoenvironmental Engineering 128, 381–390.

Griffiths, D., Fenton, G., 2001. Bearing capacity of spatially random soil: The undrained clay Prandtl problem revisited. Géotecnique 51, 351–359.

Griffiths, D.V., Fenton, G., Manoharan, N., 2002. Bearing capacity of rough rigid strip footing on cohesive soil: probabilistic study. Journal of Geotechnical and Geoenvironmental Engineering 128, 743–755. doi:10.1061/(ASCE)1090-0241(2002)128:9(743).

Hashin, Z., Shtrikman, S., 1962. A variational approach to the theory of the effective magnetic permeability of multiphase materials. Journal of Applied Physics 33, 3125. doi:10.1063/1.1728579.

Helton, J., Johnson, J., Sallaberry, C., Storlie, C., 2006. Survey of sampling-based methods for uncertainty and sensitivity analysis. Reliability engineering and system safety 91, 1175–1209.

Honjo, Y., 1985. Dam Filters: Physical Behavior, Probability of Malfunctioning and Design Criteria. Ph.D. thesis. Massachusetts Institute of Technology, Department of Civil Engineering. Massachusetts.

Honjo, Y., Otake, Y., 2013. A simple method to assess the effect of soil spatial variability on the performance of a shallow foundation, in: Withiam, J.L., Phoon, K.K., Hussein, M.H. (Eds.), Foundation Engineering on the Face

of Uncertainty, ASCE. pp. 385–402. doi:{10.1061/9780784412763.030}. geotechnical Special Publication No. 229 Honoring Fred. H. Kulhway.

Hughes, J., Haran, M., Caragea, P., 2011. Autologistic models for binary data on a lattice. Environmetrics 22, 857–871. doi:10.1002/env.1102.

ISSMGE-TC304, 2021. State-of-the-art review of inherent variability and uncertainty in geotechnical properties and models. doi:10.53243/R0001.

Jones, A., Kramer, S., Arduino, P., 2002. Estimation of Uncertainty in Geotechnical Properties for Performance-Based Earthquake Engineering. PEER Report 2002/16. Pacific Earthquake Engineering Research Center. University of California, Berkeley.

Kalender, A., Sonmez, H., Medley, E., Tunusluoglu, C., Kasapoglu, K.E., 2014. An approach to predicting the overall strengths of unwelded bimrocks and bimsoils. Engineering Geology 183, 65–79. doi:10.1016/j.enggeo.2014.10.007.

Kasama, K., Whittle, A., Zen, K., 2012. Effect of spatial variability on the bearing capacity of cement-treated ground. Soils and Foundations 52, 600–619. doi:10.1016/j.sandf.2012.07.003.

Kirkpatrick, S., 1973. Percolation and conduction. Reviews of modern physics 5, 574–588.

Li, J., Tian, Y., Cassidy, M., 2015. Failure mechanism and bearing capacity of footings buried at various depths in spatially random soil. Journal of Geotechnical and Geoenvironmental Engineering 141, 1–11.

Lindquist, E.S., 1994. The strength and deformation properties of melange. Ph.D.. University of California, Berkeley. Ann Arbor, United States. ISBN: 9798208551073.

Medley, E., 2001. Orderly characterization of Chaotic franciscan melanges. Felsbau 19, 20–33.

Medley, E.W., Sanz Rehermann, P.F., 2004. Characterization of Bimrocks (Rock/Soil Mixtures) With Application to Slope Stability Problems, in: EUROCK 2004 and 53th Geomechanics Colloquium, Salzburg, Austria.

Medley, E.W., Zekkos, D., 2011. Geopractitioner approaches to working with antisocial mélanges. Special Paper of the Geological Society of America 480, 261–277. doi:10.1130/2011.2480(13).

Montoya-Araque, E.A., Suarez-Burgoa, L.O., Medley, E.W., 2020. Application of the tortuous surface method to stochastic analysis of bimslope stability. Bulletin of Engineering Geology and the Environment 79, 5329–5340. URL: http://dx.doi.org/10.1007/s10064-020-01909-5, doi:10.1007/s10064-020-01909-5.

Montoya-Noguera, S., Lopez-Caballero, F., 2016. Numerical modeling of discrete spatial heterogeneity in seismic risk analysis: Application to treated ground soil foundation. GeoRisk: Assessment and Management of Risk for Engineered Systems and Geohazards 10, 66–82. doi:10.1080/17499518.2015.1058957. special issue: Modeling spatial variability in Geotechnical Engineering.

Napoli, M.L., Festa, A., Barbero, M., 2022. Practical classification of geotechnically complex formations with block-in-matrix fabrics. Engineering Geology 301, 106595. URL: https://linkinghub.elsevier.com/retrieve/pii/S0013795222000801, doi:10.1016/j.enggeo.2022.106595.

Napoli, M.L., Milan, L., Barbero, M., Scavia, C., 2020. Identifying uncertainty in estimates of bimrocks volumetric proportions from 2D measurements. Engineering Geology 278, 105831. doi:10.1016/j.enggeo.2020.105831.

Nobahar, A., 2003. Effects of soil spatial variability on soil-structure interaction. Ph.D. thesis. Memorial University of Newfoundland. Canada.

Nobahar, A., Popescu, R., 2000. Spatial variability of soil properties – effects on foundation design, in: Proceedings of 53rd Canadian geotechnical conference, Montreal, Quebec. pp. 1139–1144.

Phoon, K.K., Kulhawy, F., 1999. Evaluation of geotechnical property variability. Canadian Geotechnical Journal 36, 625–639. doi:10.1139/t99-039.

Popescu, R., Deodatis, G., Nobahar, A., 2005a. Effects of random heterogeneity of soil properties on bearing capacity. Probabilistic Engineering Mechanics 20, 324–341. doi:10.1016/j.probengmech.2005.06.003.

Popescu, R., Prevost, J.H., Deodatis, G., 2005b. 3D effects in seismic liquefaction of stochastically variable soil deposits. Géotechnique 55, 21–31.

Prandtl, L., 1921. Uber die Eindringungsfestigkeit (Harte) plastischer Baustoffe und die Festigkeit von Schneiden. Zeitschrift fur angewandte Mathematik und Mechanik 1, 15–20.

Schmüdderich, C., Prada-Sarmiento, L.F., Wichtmann, T., 2021. Numerical analyses of the 2D bearing capacity of block-in-matrix soils (bimsoils) under shallow foundations. Computers and Geotechnics 136, 104232. URL: https://linkinghub.elsevier.com/retrieve/pii/S0266352X21002305, doi:10.1016/j.compgeo.2021.104232.

Sonmez, H., Kasapoglu, K.E., Coskun, A., Tunusluoglu, C., Medley, E.W., Zimmerman, R.W., 2009. A Conceptual empirical approach for the overall strength of unwelded bimrocks, in: Regional Symposium in Rock Engineering in difficult ground conditions, soft rock and Karst, ISRM, Dubrovnik, Croatia. pp. 29–31.

Suarez-Burgoa, L.O., Ariza-Triana, A., Montoya-Araque, E., 2019. Modelamiento de estructuras de bimsoils mediante el empaquetado de partículas circulares en r^2. $Revistadela Facultadde Ciencias 8, 115 - -137. doi : .$

Vanmarcke, E., 1977. Probabilistic modeling of soil profiles. Journal of the Geotechnical Engineering Division 103, 1227–1246.

Wang, J.P., Huang, D., 2012. RosenPoint: A Microsoft Excel-based program for the Rosenblueth point estimate method and an application in slope stability analysis. Computers & Geosciences 48, 239–243. 10.1016/j.cageo.2012.01.009.

Wang, Y., Cao, Z., Li, D., 2016. Bayesian perspective on geotechnical variability and site characterization. Engineering Geology 203, 117–125. http://dx.doi.org/10.1016/j.enggeo.2015.08.017, 10.1016/j.enggeo.2015.08.017. publisher: Elsevier B.V.

Whittle, P., 1963. Stochastic processes in several dimensions. Bulletin of the International Statistical Institute 40, 974–994.

Wiener, O., 1912. Die theorie des Mischkorpers fur das feld des stationaren Stromung. Erste Abhandlung die Mittelswertsatze fur Kraft, Polarisation un Energie. (german) [The theory of composites for the field of steady flow. First treatment of mean value estimates for force, polarization and energy]. Abhandlungen der mathematisch-physischen Klasse der Koniglich Sachsischen Gesellschaft der Wizzenschaften 32, 509–604.